POLITECNICO DI TORINO
Repository ISTITUZIONALE

Functionalization and use of grape stalks as poly(butylene succinate) (PBS) reinforcing fillers

Original
Functionalization and use of grape stalks as poly(butylene succinate) (PBS) reinforcing fillers / Nanni, A., Cancelli, U., Montevecchi, G., Masino, F., Messori, M., Antonelli, A.. - In: WASTE MANAGEMENT. - ISSN 0956-053X. - 126:(2021), pp. 538-548. [10.1016/j.wasman.2021.03.050]

Availability:
This version is available at: 11583/2896103 since: 2021-04-20T16:43:58Z

Publisher:
Elsevier Ltd

Published
DOI:10.1016/j.wasman.2021.03.050

Terms of use:

This article is made available under terms and conditions as specified in the corresponding bibliographic description in the repository

Publisher copyright
Elsevier postprint/Author's Accepted Manuscript

© 2021. This manuscript version is made available under the CC-BY-NC-ND 4.0 license
http://creativecommons.org/licenses/by-nc-nd/4.0/.The final authenticated version is available online at:
http://dx.doi.org/10.1016/j.wasman.2021.03.050

(Article begins on next page)

09 November 2026

Functionalization and use of grape stalks as poly(butylene succinate) (PBS) reinforcing fillers

Alessandro Nanni[a], Umberto Cancelli[b], Giuseppe Montevecchi[b,*], Francesca Masino[b], Massimo Messori[a], Andrea Antonelli[b]

[a] Department of Engineering Enzo Ferrari, University of Modena and Reggio Emilia, Via Pietro Vivarelli 10, Modena, Emilia-Romagna, 41125, Italy

[b] Department of Life Sciences (Agri-Food Science Area), BIOGEST - SITEIA Interdepartmental Centre, University of Modena and Reggio Emilia, Piazzale Europa 1, Reggio Emilia, Emilia-Romagna, 42124, Italy

Corresponding author: Giuseppe Montevecchi

E-mail address: giuseppe.montevecchi@unimore.it (G. Montevecchi).

ABSTRACT: Grape stalks are a lignocellulosic biomass, which is a very complex material, whose easy and profitable fractionation to obtain its basic components is still not available. Therefore, alternative ways to try and make use of grape stalks are currently being explored.

In the present study, the possible use of dried and milled grape stalks as filler in bio-composites was assessed using polybutylene succinate as a basic polymer. The tensile specimens produced using 10% grape stalk powder as it is and functionalized through pre-extrusion acetylation and silylation, and silylation *in situ* were characterized for their structural, mechanical, thermal, morphological, and color properties. The bio-composites showed to be stiffer than the control polymer, with an increase of Young's modulus from 616 MPa to 732 MPa in the specimens obtained with acetylated grape stalk powder.

This led to a potentially new method to valorize by-products of the wine industry such as grape stalks in order to recover raw materials which could prove useful in the biomaterials and bio-composites sector.

KEYWORDS: wine chain; by-product; lignocellulosic biomass; composites; biopolymers.

1. Introduction

The increase of the world population and the corresponding growth in consumption has led in recent years to an expansion of industrial activities in order to produce goods and services, especially in the agro-industrial sector (Brandt et al., 2013, Lieder and Rashid, 2016, Maina et al., 2017, Nanni et al., 2021). This involves the issues of accumulation and disposal of by-products present at various cycles of the food chain (Gustavsson et al., 2011).

Nowadays, one of the strategies most used to reduce the socio-economic and environmental impact of by-products in the production chain is the creation of closed systems (Parisi et al., 2021, Ravindran and Jaiswal, 2016). Indeed, the circular economy allows by-products, which would otherwise end up as waste, to be converted into secondary raw materials. In the logic of a regenerative approach, these materials can be returned to the various production cycles for the creation of value-added products (MacArthur, 2013, Stegmann et al., 2020).

The grapevine is one of the most cultivated crops in Italy and the plains and hills of the Emilia-Romagna region, in Northern Italy, are particularly devoted to this practice. Here, grapes are mainly intended for the production of wine, however other products derived from grapes, such as enocyanin from Ancellotta, vinegar, balsamic vinegar, concentrated musts, and traditional garnishes contribute to the issue of the accumulation of by-products (Masino et al., 2008, Montevecchi et al., 2011, Montevecchi et al., 2014, Vasile Simone et al., 2013).

In particular, the management of grape stalks, grape pomace, yeast lees, and wastewater remains an unsolved problem (Barba et al., 2016, Cancelli et al., 2020). According to some data deriving from the calculation of the carbon footprint of Italian winemaking,

the equivalent CO_2 emissions in 2016 were 834,300 tons for grape pomace and 185,400 for grape stalks (Bevilacqua et al., 2017, Lucarini et al., 2018). These latter are extraordinarily recalcitrant for employment in convenient applications and, for this reason, they are still highly underutilized.

The presence of resistant fibrous biopolymers in the structure of lignocellulosic biomass makes it interesting as a reinforcing filler in the realization of bio-composite materials (Ghaffar et al., 2015, Hernandez Michelena, 2019). Bio-composites produced through the incorporation of a filler deriving from food by-products into a biodegradable and biobased polymer are nowadays among the most interesting materials for future applications in the sector of bioplastics and packaging (Bharath and Basavarajappa, 2016, Fortea-Verdejo et al., 2017, Nanni and Messori, 2020a, Nanni et al., 2020, Seggiani et al., 2015, Seggiani et al., 2016). In particular, lignocellulosic fibers have many advantages such as low cost, non-toxicity, biodegradability, and easy availability (Kalia et al., 2013).

Among the most interesting polymers nowadays available in the market, polybutylene succinate (PBS) is an aliphatic polyester that, thanks to its mechanical properties similar to the ones of polypropylene and polyethylene (Hernandez Michelena, 2019, Luzi et al., 2019), can find space in many applications such as agriculture, packaging films, and consumer's goods. Moreover, PBS is highly sustainable, as its building blocks are partially bio-based. In the last years, its monomers, namely 1,4-butanediol and succinic acid, have been synthesized also through fermentation of agro-industrial derived sugars (Yeh et al., 2010, Yim et al., 2011, Zeikus et al., 1999), and it is also fully biodegradable; thus, its use could reduce the consumption of fossil fuels and tackle the problems relating to plastic pollution at the same time. Therefore, the possibility to use

grape stalks as PBS reinforcing filler is very intriguing since they would simultaneously increase the PBS bio-based content and offer a new opportunity of waste valorization to wine-sector companies.

As for possible preliminary treatments to improve the characteristic of the finished product, chemical functionalization of the grape stalk powder has already been successfully used to increase the adhesion between the hydrophobic polymer and the polar lignocellulosic matrix (Abdellaoui et al., 2018, Espert et al., 2003, Gwon et al., 2010a). Acetylation and silanization are two common techniques to cap hydroxyl groups and ease the creation of hydrophobic interactions between the functionalized lignocellulose and the polymer (Gwon et al., 2010a). Furthermore, the functionalization of the lignocellulosic structure increases its stability against moisture and biodeterioration (Mohammed-Ziegler et al., 2008).

The general aim of this project is to explore alternative solutions for the technical and commercial valorization of grape stalks. In particular, in the Emilia-Romagna region where we conducted this study, and specifically in the provinces of Modena and Reggio Emilia, the amount of grape stalks used for the production of biogas and composted digestate can be up to 2800 t/year (Ronga et al., 2019). Although grape stalks are partially used for livestock feeding (Maicas and Mateo, 2020), the highest amount is either destined to landfills or it is left to accumulate on the soil with consequent phytotoxicity problems caused by the phenolic compounds to the microbiota (Troncozo et al., 2019).

For these reasons, the purpose of this study is the production and evaluation of grape stalk powder as a filler for biocomposite production using PBS as a basic polymer. Grape stalks powder was also used in its functionalized forms through acetylation and

110 silanization. The structural, mechanical, thermal, and color properties were measured to
111 ascertain the potential replacement of a part of PBS in order to obtain the least possible
112 loss of performance.
113
114 **2. Experimental**
115 ***2.1. Chemicals***
116 Acetic anhydride, ethanol, pyridine, and toluene were supplied by Sigma-Aldrich
117 (Milan, Italy). The paraffinic oil "Vestan" was provided by Tizi S.r.l. (Arezzo, Italy),
118 while Geniosil GF 31 3-trimethoxysilylpropyl 2-methylprop-2-enoate (MPTMS, CAS
119 2530-85-0) came from Wacker Chemical Corporation (Milan, Italy). Deionized water
120 was obtained through an Elix^{3UV} purification system (Merck Millipore, Milan, Italy).
121
122 ***2.2. Sampling, drying, and milling to obtain a fine powder***
123 Grape stalks (200 kg), collected from some wine cellars in the provinces of Modena and
124 Reggio Emilia, were first cleaned to remove residues of grape skins and grape seeds and
125 then oven-dried at 65 °C (24-48 h) up to constant weight. Then, the dried grape stalks
126 were subjected to milling (universal cutting mill, Pulverisette 19, Fritsch Gmbh, Idar-
127 Oberstein, Germany) in order to considerably reduce the dimensions of the material.
128 The result obtained was a fine powder with a high surface area, thus facilitating the
129 subsequent treatments of the material. The powder was then sieved to separate it into
130 the following mesh classes: 63 μm, 212 μm, 500 μm, and 850 μm. The various sieves
131 (Giuliani Tecnologie S.r.l., Torino, Italy) were stacked in decreasing order of mesh size.
132 The powder was placed on the first sieve with a mesh size of 850 μm and through a
133 vibratory movement the various fractions separated and settled down on different levels

according to the particle size. The fraction of the powder taken into consideration for the realization of bio-composite materials was that of a particle size between 63 and 212 µm.

2.3. Functionalization through acetylation

This fraction was subjected to an acetylation reaction (Fig. S1a) and an aliquot of 50.00 g of the powder was weighed and introduced into a 1-L flask with 500 mL of acetic anhydride and 50 mL of pyridine (Hussain, 2004). The reaction flask was immersed in a silicone oil bath under continuous stirring for about 3 h at 160 °C. The material was then filtered by the Bückner apparatus and thrice washed with 30 mL of ethanol to remove the reagents. The solid residue recovered was dried in a stove at 65 °C for two days.

2.4. Functionalization through silanization

The same fraction of powder was subjected to the silanization reaction with MPTMS as a derivatizing reagent (Fig. S1b) to modify the lignocellulose structure by forming C-O-Si ester bonds (Abdellaoui et al., 2018, Hernandez Michelena, 2019). An aliquot of 25.00 g of grape stalk powder was dispersed in 25.00 g of toluene and 24.84 g of MPTMS was added to this mixture (Brostow et al., 2016). The sample was then washed with toluene and filtered by a Bückner funnel and the solid residue recovered from this mixture was dried at 70 °C for 24 h. The yields of the two reactions were determined.

2.5. Fourier-Transform Infrared Spectroscopic (FT-IR) analysis

157 The obtained three fractions (grape stalk powder as it is, acetylated and silylated
158 powders) were subjected to the attenuated total reflectance Fourier-transform infrared
159 spectroscopic analysis (ATR-FT-IR, Vertex 70, Bruker, Milan, Italy). The instrument
160 was equipped with a Golden Gate™ (Specac) high-performance single reflection
161 monolithic diamond sampling accessory, featuring a Type IIIA diamond ATR element
162 metal-bonded into a tungsten carbide mount. Data were collected using OPUS software
163 v6.5 (Bruker). For each sample, 32 spectra were obtained and co-added for each sample
164 at a resolution of 4 cm^{-1}. A background spectrum was obtained by collecting 32 co-
165 added scans after the crystal was cleaned with acetone.
166
167 ***2.6. Bulk density and particle density***
168 The bulk density (including the contribution of the inter particulate void volume) of the
169 samples was measured with the 10 mL graduated cylinder, while the particle density (or
170 true density, that is the mass of a particle divided by its volume, excluding open and
171 closed pores) was measured using a pycnometer AccuPyc 1330 (WHO, 2012).
172
173 ***2.7. Procedure for the production of bio-composite materials***
174 Firstly, 150 g of PBS and 1.5 g of paraffin oil were manually mixed to make the
175 polymer wet and sticky, thus improving the adhesion between grape stalks and pellets
176 surface as well as the polymer-filler homogeneity before extrusion. Subsequently, 15 g
177 of grape-stalk fractions were added to the polymer (concentration of 10 parts for
178 hundred parts of rubber, phr). Four different fractions were used: (i) grape stalk powder
179 as it is (PBS 10GS), (ii) acetylated powder (PBS 10AcGS), and (iii) silylated powder
180 (PBS 10SilGS). A variant of PBS 10SilGS was prepared by mixing in the extruder 1 phr

of silane with 150 g PBS and with 10 phr of untreated grape stalks powder in order to obtain (iv) a silanization *in situ* (PBS 10SilSituGS) sample. The different formulations were extruded with a twin-screw extruder (557 Rheomex, Haake S.r.l., Rezzato BS, Italy) using the following temperatures (feed zone, barrel, and die): 80, 120, and 125 °C and a screw speed of 50 rpm. The extruded materials were air-cooled, manually spooled, and then granulated. The four granulates were processed by injection molding machine (MegaTech TecnicaDueBi injection molding machine, Fabriano, Italy) in order to obtain specimens for the mechanical analysis of the bio-composite materials, for the color measurements, and for the morphological and infrared spectroscopic analysis (Seggiani et al., 2017). Injection molding was conducted using a temperature profile ranging from 90 °C (hopper zone) to 170 °C (die zone), a holding pressure of 40 bar, a holding time of 3 sec and a cooling step of 6 sec. As a comparative reference, PBS was also processed under the same conditions mentioned above (PBS proc).

2.8. Scanning electron microscope - Field emission gun (SEM-FEG)

A scanning electron microscope (Nova NanoSEM 450, SEM-FEG, FEI Europe B.V., Hillsboro, USA), operating in low-vacuum conditions and equipped with a microanalysis X-EDS detector (QUANTAX-200, Bruker Corporation, Billerica, USA) was used to analyze the morphology of the PBS-based samples as well as of both untreated and treated grape stalks powders. In the case of PBS-based specimens, they were broken down into liquid nitrogen and the cross-section surface was observed, while in the case of grape stalks powder, they were directly observed after drying.

2.9. Thermogravimetric analysis

Thermogravimetric analysis (TGA) was carried out to evaluate the thermal stability of the grape stalks' powders and of the PBS-based composites. Tests were conducted on 15 ± 2 mg of each sample in a Perking-Elmer TGA 4000 instrument (Waltham, USA), using a temperature ramp of 10 °C min^{-1} from 40 °C to 600 °C under inert atmosphere (nitrogen flow of 40 mL min^{-1}).

The moisture uptake (MU) content was evaluated as the percentage decrease of the filler mass between 40 and 100 °C. T_5 and T_{15} were obtained from the thermograms as the temperatures at which the samples exhibited a mass loss of 5 and 15%wt., respectively, while R_{600} was obtained as the residual percentage mass of the sample evaluated at 600 °C. The degradative peak temperatures (T_{peak}) were calculated as the temperatures at which the maximum derivative weight with respect to temperature (differential thermal analysis, DTA) occurred. In addition, the TGA data obtained from grape stalks powders and from PBS-based composites were fitted to the mathematical model proposed by Nabinejad et al. (2015) in order to determine the effective amount of GS filler (P_f) present within PBS-based composites. The idea behind this model is that by increasing the filler loading, the thermogravimetric (TG) behavior of the composite material would become more and more similar to the behavior of the neat filler. The actual amount of filler within composites is very important since it provides indications on the processing capacity of the formulation and allows for a finer discussion of the composites' mechanical properties. In this context, the actual GS filler contents (P_f) obtained were used as an input for the micro-mechanical models described in the next section. The model proposed by Nabinejad et al. (2015) is based on the following formula:

$$P_f(\%) = \alpha m_{dc} + \beta R_{600,c} \quad (1)$$

where P_f represents the effective mass percentage of the filler within the composite, m_{dc} is the percentage mass loss of composite evaluated at the T_{peak} of the filler, and $R_{600,c}$ is the percentage mass residue of the composite at 600 °C. The mass drop coefficient α and the mass residue coefficient β can be calculated as follows:

$$\alpha(-) = \frac{R_{600,p}}{R_{600,p}M_{df} - R_{600,f}M_{dp}}100 \quad (2)$$

$$\beta(-) = \frac{-M_{dp}}{R_{600,p}M_{df} - R_{600,f}M_{dp}}100 \quad (3)$$

where $R_{600,f}$ and $R_{600,p}$ are the percentage mass residues evaluated at 600 °C of the neat filler and of the neat polymer, respectively, while M_{df} and M_{dp} are the percentage mass decreases of the neat filler and polymer evaluated at $T_{peak,f}$.

2.10. Mechanical properties and micro-mechanical analysis

Tensile tests were performed using a dynamometer (5567, Instron, Pianezza, Italy) equipped with a load cell of 1 kN and an extensometer of 25 mm. Tests were conducted with a 10 mm/min clamp separation speed. Young's modulus (E), tensile strength (σ_M), and elongation at break (ε_b) values were reported as the average of ten measurements. The intrinsic stiffness of grape stalks fibers (E_P) was obtained by applying two micromechanical models often used for the prediction of the Young's modulus of composites (E_C), namely the Voigt model (1889) and the Halpin-Tsai model (Halpin, 1969). The Voigt equation is generally used to predict the elastic modulus of composite materials where reinforcing fibers are supposed to be disposed in a parallel direction to the axial loading (Voigt, 1889) (parallel model). The Halpin-Tsai model is used to predict, in a simple and semi-empirical manner, the moduli of composites reinforced by short aligned fibers. In spite of the fact that these models do not account for many

252 factors such as the variability in the modulus of constituents and the effect of the
253 compounding process (Battegazzore et al., 2019), they have already been successfully
254 applied to estimate the elastic modulus of several natural fillers/fibers (Ahankari et al.,
255 2011).
256 Similarly, Pukanszky's equation (Pukanszky, 1990), which is generally used to predict
257 the tensile strength of composite materials filled with short-fibers or quasi-spherical
258 fillers, was applied to the tensile strength data of PBS-based samples to obtain the
259 empirical adhesion B factor. The adhesion B factor is a useful tool to quantify and
260 compare the effectiveness of the particle-matrix adhesion in different composites. The
261 mentioned equations are reported as follows:
262 $$Voigt: E_C = E_P V_P + E_M(1 - V_P) (4)$$
263 $$Halpin - Tsai: E_C = E_M \frac{1 + 2\eta V_P}{1 - \eta V_P} with \eta = \frac{\frac{E_P}{E_M} - 1}{\frac{E_P}{E_M} + 2} (5)$$
264 $$Pukanszky: \sigma_C = \sigma_M \frac{1 - V_P}{1 + 2.5V_P} expexp(BV_P) (6)$$
265
266 where E_C is the composite modulus, E_M is the polymer matrix modulus, E_P is the filler
267 particle modulus, V_P is the filler particle volume fraction, σ_C is the composite tensile
268 strength, σ_M is the polymer matrix tensile strength and B is the Pukanszky's empirical
269 adhesion constant.
270 TA DMA Q800 instrument was used in the single cantilever flexural configuration to
271 evaluate the dynamic mechanical behavior of the different PBS-based samples
272 exploiting rectangular specimens with the following sizes (l, w, t); 17 × 5 × 2 mm^3.

DMA tests were run with a heating rate of 3 °C/min from -40 to 100 °C with the oscillation frequency and the strain set at 1 Hz and 0.1%, respectively.

For each sample, the storage modulus (E') and the tan δ (damping factor) (Saba et al., 2016) were plotted as temperature's functions while the glass transition temperature (T_g) was evaluated as the temperature at which the maximum tan δ value was observed.

2.11. Thermal properties

The thermal properties of the PBS-based samples were evaluated by Differential Scanning Calorimetry (DSC) (DSC TA 2010). DSC measurements were performed using 10 ± 2 mg of sample and 50 mL/min of nitrogen as purging gas. Each sample was first heated up to 200 °C at 15 °C/min in order to erase the previous thermal history. Subsequently, samples were cooled to 0 °C at 10 °C/min and re-heated to 200 °C at 10 °C/min. Crystallization temperature (T_C) and crystallization enthalpy (H_C) were evaluated during the cooling cycle meanwhile melting temperature (T_m) and melting enthalpy (H_m) were assessed from the second heating cycle. The crystallinity percentage (χ) was determined considering the weight fraction occupied by the additives and the value of 110 J/g as a reference for the 100% crystalline PBS melting enthalpy (Xu and Guo, 2010).

2.12. Color measurements

CIELab coordinates (L*, a*, b*) were measured on the functionalized powder samples and specimens through a tristimulus colorimeter (Chroma Meter CR-400, Konica Minolta, Milan, Italy) in transmittance mode over the visible spectrum (from 380 to 770 nm), using the illuminate D65 and 10° standard observer (McLaren, 1976). Chroma (C),

hue (H), and color distance (CD) were calculated according to the formula described by Hunt and Pointer (2011).

2.13. Statistical analysis.

Univariate analyses were carried out on the data set. Differences among varieties were assessed by analysis of variance (one-way ANOVA) based on three replicates for each sample. When a significant effect (at least $p \leq 0.05$) was shown, comparative analyses were carried out by the post hoc Tukey's multiple comparison test. All tests were performed with Statistica v8.0 software (Stat Soft Inc., Tulsa, USA).

3. Results and discussion

3.1. Yields and physical characterization of the functionalized grape stalk powders

Grape stalks are lignocellulosic materials with a reported composition of cellulose (20-30%), hemicellulose (15-25%), lignin (20-30%), tannins (around 16%) and ashes (4-6%) (Prozil et al., 2012, Prozil et al., 2014, Spigno et al., 2013). All these compounds are characterized by the strong presence of hydroxyl groups, which well-lend themselves to chemical derivatization reactions used to obtain more lipophilic lignocellulose structures which, in turn, display an improved interaction with PBS polymer chains.

The grape stalk powder as it is and those functionalized were tested as fillers for the realization of bio-composite materials with polybutylene succinate. The powder subjected to acetylation reaction gave a yield of 31.19 g (62%) starting from 50.00 g of raw material, while the one treated by silanization yielded 24.34 g starting from 25.00 g of initial material.

320 The bulk density and particle density (or true density) measurements are shown in Table
321 1. The functionalized samples showed significantly lower density values ($p \leq 0.01$) as
322 compared to the untreated powder, thus confirming their decrease as the subsequent
323 effect of the derivatization reaction. This can be explained by the breakdown of the
324 intra- and intermolecular hydrogen bonds, which are usually responsible for the native
325 configurations of cellulose and hemicellulose macromolecules (Jarvis, 2018).
326 The structural analysis of the derivatized grape stalk powder was carried out with FT-IR
327 spectroscopy to highlight different functional groups between the control sample and
328 the modified ones. Fig. 1a shows the infrared spectra of the control sample as it is, the
329 acetylated and the silylated powders. In the FT-IR spectrum of the control sample, the
330 band relating to the stretching of the hydroxyl group (3330 cm^{-1}) appeared to be
331 relevant, while in the spectrum of the corresponding material functionalized through
332 acetylation this band was almost absent. Conversely, the band relating to the stretching
333 of the carbonyl group (1720 cm^{-1}) showed a significant increase as a consequence of the
334 acetylation reaction. Similar considerations cannot be done for silylated powder,
335 probably due to the poor reactivity of the silylating reagent towards the grape stalk
336 powder.
337 From a morphological point of view, the SEM images of the surface of both untreated
338 and treated grape stalk powders were reported in Fig. 1b, 1c, and 1d. Looking at the
339 untreated grape stalk powder (Fig. 1b), many surface impurities can be observed,
340 especially close to the edges of the GS particles and fibers. On the contrary, Fig. 1c
341 shows that acetylation reaction removed nearly all the impurities from the particle and
342 fiber surface. Indeed, during acetylation, waxy substances of fibers/particles are
343 dissolved and hydroxy groups are replaced by acetyl groups, as other similar works also

reported (Le Troedec et al., 2008, Pickering et al., 2007, Tserki et al., 2005). In addition, SEM micrographs also show that the surfaces of the acetylated grape stalks were rougher and spongier than those of the untreated grape stalks. This behavior, which can be explained by the esterification reactions leading to higher surface roughness and porosity (Li et al., 2007), is a positive feature since rougher surfaces have higher chances of mechanically interlocking with polymer chains during melt compounding (Hajiha et al., 2014). The SEM images of grape stalks before and after silane treatment (Fig. 1b and 1d, respectively) are not significantly different in terms of morphology. Similar results were also reported by other studies on silanization of fibers, where the surface morphology was not found to have been modified by the -OH group silanization (Sawpan et al., 2011, Suardana et al., 2011). Nevertheless, it can be noticed that silylated grape stalks have fewer impurities on their surface compared to untreated grape stalks. It is noteworthy to notice that elemental analysis of silylated grape stalks obtained through X-EDS (Fig. S2c) showed the presence of silicon (around 1%wt.) in the fibers/particles, which proves its successful reaction.

Finally, the TGA data (under nitrogen atmosphere) of untreated and treated grape stalks are shown in Table 1 and in Fig. S3. It can be noticed that GS and SilGS exhibited a similar behavior in terms of thermal stability. Both samples exhibited two peaks of degradation (peak 1 and peak 2 of the DTA curves); the first one occurred at around 193 °C, while the second one at 309 °C. From a qualitative point of view, the first degradative peak can be associated to the loss of the hemicellulose fraction, which is less stable than cellulose and lignin (the latter being the most stable of the two) (Ramiah, 1970), while the second degradative peak can be attributed to the loss of cellulose. Conversely, AcGS (Fig. S3b) only showed a single marked mass loss step at

around 344 °C, while peak 1 was almost absent. It is reasonable to suppose that AcGS exhibited only a slight first degradative peak because the hemicellulose fraction could have been depolymerized under the strong conditions of acetylation reaction (Zhao et al., 2020). This hypothesis has been partially confirmed by the FT-IR spectra reported in Fig. 1a where the –OH peak of AcGS is much less marked than in GS and SilGS. As a consequence, AcGS seems to be the most stable powder, a finding which has also been confirmed by the T_{15} value (the temperature at which 15% of mass loss is observed) which was roughly 30 °C higher than the values found in GS and SilGS.

From an application point of view, the T_{15} of each tested powder was much higher than the PBS processing temperatures, thus confirming the possibility of exploiting grape stalks as natural fillers within PBS. Looking at the final part of the TG curves, GS and SilGS exhibited residues values (R_{600}) almost two times higher than AcGS. Again, this result can be explained by the fact that the hemicellulose was partially removed during the acetylation reaction. Finally, a reduction from 38% (SilGS) to 48% (AcGS) in moisture uptake was found in treated grape stalks, thus confirming the hydrophilicity reduction in grape stalks following surface treatments. This aspect is particularly important from an application point of view since fillers need to be dried before they can compound with bio-polyesters in order to avoid possible degradative hydrolysis reactions of the polymer chains.

3.2. Thermal properties of the bio-composites

The thermal properties (T_g, T_c, T_m, and χ) of the PBS-based samples, evaluated by Differential scanning calorimetry (DSC), are reported in Table 2. No significant differences in the thermal behavior of PBS were showed by adding grape stalks as

392 fillers. Moreover, also the typology of the surface treatment did not exhibit any
393 particular behavior. Considering the melting and crystallization temperatures (T_m and
394 T_c), the maximum deviations were observed in the PBS 10SilGS sample, in which T_m
395 and T_c were lower than 0.6 and 1.5 °C, respectively, if compared with pure PBS.
396 Similarly, the PBS crystallinity appeared unchanged by the addition of grape stalks. In
397 general, when their particle size is markedly low, natural fillers can act as nucleating
398 agents, thus accelerating and increasing the formation of crystalline domains (Kai et al.,
399 2005, Väisänen et al., 2017, Zhang et al., 2012). In the present case, the unchanged
400 crystallinity pointed out the necessity to further optimize the grinding step in order to
401 enhance the crystal domain. Nevertheless, the grape stalk particles were not too coarse,
402 as testified by the fact that crystallinity was not decreased. Indeed, when using too gross
403 fillers, the agglomeration phenomena can inhibit the crystallization (Nanni and Messori,
404 2020a).
405 In order to evaluate the thermal stability of the PBS-based composites,
406 thermogravimetric analysis (TGA) was conducted by heating samples taken from the
407 tensile specimens from a starting temperature of 40 °C up to 600 °C under inert
408 atmosphere (nitrogen). The obtained TG and DT curves and data are reported in Fig. 2
409 and in Table 2, respectively. Neat PBS degraded in one fast mass loss step between 300
410 and 400 °C, as other authors have also reported (Chrissafis et al., 2005, Nanni et al.,
411 2020). Looking at Fig. 2a, it is evident that the same degradative behavior was also
412 observed in PBS samples filled with grape stalks. Nevertheless, in composites, the TG
413 curves had shifted to the left (lower temperatures) of about 20-30 °C. In particular, the
414 T_5 temperatures (temperatures at which 5% of mass loss is reached) of PBS-based
415 composites were particularly lower compared to the temperature of neat PBS (around -

44 °C in the case of GS and SilGS) and this fact can be explained by the intrinsic lower thermal stability of the hemicellulose fraction present within grape stalks. These earlier mass losses do not represent an application problem since the T_5 temperatures were much higher than the processing conditions of PBS polymer. Moreover, looking at the values of T_{15}, which is generally used as reference for the maximum temperature applicable to a polymer, no differences among filled and neat PBS are evident. From a comparative point of view, PBS 10AcGS sample exhibited the higher T_5 value, which is in perfect agreement with the intrinsic higher thermal stability of the acetylated grape stalks (Table 1). Finally, TG data were also fitted with equations 1-3 to evaluate the actual content of the filler within the composite (P_f). As reported in Table 2, the mathematical model reported an actual amount of filler consistent with the processed formulation for all samples except for PBS 10SilSitu. In this case, the model showed that only 6.2%wt. of grape stalks were present within the PBS matrix. This data is reasonably correct because, as further shown, both the TG and the mechanical data of PBS 10SilSitu are midway in between the ones of neat PBS and 10%wt. filled composites, thus implying it has a mid-term content of filler. It is fair to suppose that, during reactive extrusion, grape stalks, with the aid of sticky silane, formed aggregates which were not transported by the screws of the extruder; further work should verify this hypothesis.

The actual filler content resulting from the model was used as an input to obtain other micro-mechanical parameters, as the section 3.3 shows. All parameters of equations 1-3 are available in the supplementary data file.

3.3. Tensile properties of the bio-composites

In Table 2 and in Fig. S4, the tensile properties of the bio-composites are reported. In each case, the grape stalks enhanced the pure PBS Young's modulus of around 17-18%. Such an increase in stiffness could be linked to the hydrophobic interactions as well as to the hydrogen-bonds electrostatic forces occurring between the modified lignocellulosic material and the co-polymer (Bharath and Basavarajappa, 2016, Mu et al., 2018). The functionalization of lignocellulosic fiber led to an increase in the contact interfaces between the copolymer and the lignocellulosic filler (Borsoi et al., 2019, Gwon et al., 2010b).

Nevertheless, Young's modulus is only moderately affected by the particle-polymer adhesion since this property is evaluated at low deformations in which separation phenomena of particle-matrix interface generally do not occur (Fu et al., 2008, Nanni and Messori, 2020a). This hypothesis is also supported by the fact that even PBS 10GS (untreated grape stalks) showed an increased elastic modulus value. Therefore, the increase in Young's modulus is mainly explained by the fact that GS particles are intrinsically stiffer and harder than the PBS matrix. The stiffness of lignocellulosic materials such as grape stalks generally depends on the amounts of cellulose, hemicellulose and lignin they contain, since cellulose (140 GPa) is much stiffer than hemicellulose (8 GPa) while lignin normally acts as a coupling bonding agent (between cellulose and hemicellulose) rather than as stiffening element (Cousins, 1978, Gurunathan et al., 2015). Therefore, the high content of cellulose (20-30%wt.) within grape stalks could explain the gain in elastic modulus observed in the PBS-based composites. In addition, the fact that PBS 10AcGS exhibited the highest Young's modulus could be due to the degradation of hemicellulose during the acetylation reaction.

464 The GS elastic moduli (E_P), obtained by applying the theoretical models of Voigt and
465 Halpin-Tsai on the experimental data, are reported in Table 3. These models require as
466 input the filler volume of fractions (V_P), which were calculated using the actual filler
467 contents (P_f values in Table 3) and the particle densities (Table 1). The Voigt model
468 gave E_P values lower than the ones obtained using the Halpin-Tsai model although its
469 standard deviation was lower than the one observed in the Halpin-Tsai model.
470 Nevertheless, both models provided comparable E_P values and thus it can be estimated
471 that the intrinsic grape stalks Young's modulus ranges between 1.3 and 1.8 GPa. It is
472 interesting to notice that GS stiffness was lower but similar to the one reported for lees
473 filtered from the wine mass (between 1.8 and 2.5 GPa), that were tested with PBS at 10
474 phr loading (Nanni and Messori, 2020b).
475 In the case of PBS 10SilSituGS, if a filler content input of 10%wt. (V_P of 0.12) was
476 used, the Voigt and Halpin-Tsai models would have given E_P values of 1096 and 1239
477 MPa, respectively, which are considerably lower compared to the other ones. Actually,
478 using the 6.2%wt. value, the obtained E_P values (Table 3) are more consistent with the
479 others, thus pointing out the reliability of the equations 1-3 previously fitted on TGA
480 data.
481 Looking at the tensile strength data (σ_M) reported in Table 2, the presence of grape
482 stalks lowers this mechanical property of around 10-20%, compared with neat PBS.
483 However, this loss was not so dramatic if compared to other studies in which PBS bio-
484 composites showed tensile strength values 26-31% lower than pure PBS (Sahoo et al.,
485 2011, Then et al., 2013). This aspect can be explained by a good adhesion between the
486 PBS matrix and the GS particles. Indeed, in polymer composites, the tensile strength
487 mainly depends on the particle-matrix adhesion since well-bonded particles can better

transfer the stress load across the interface while poor adhesion leads to physical discontinuities unable to support mechanical loads. (Borsoi et al., 2019, Fu et al., 2008). FT-IR analysis on the biocomposites was performed, however, there were no differences in the FT-IR spectra of the various samples, and for this reason the spectra were no shown. As a matter of fact, the carbonyl band of PBS far outweighs the added one thanks to the contribution given by the acetylated grape stalks.

In Fig. 3, SEM-FEG images of PBS 10GS and PBS 10AcGS surfaces were reported in order to make a qualitative investigation of the interactions between grape stalks fillers and PBS matrix. From micrographs taken at lower magnifications (Fig. 3a and 3b), it can be noticed that grape stalks fillers were homogeneously distributed and well dispersed through the surface of both composites. By increasing the magnification (Fig. 3c and 3d), it is possible to notice that acetylated grape stalks were well connected with the PBS matrix and that adhesion problems were not detectable. This positive behavior, indirectly proved by the high tensile strength values, is the consequence of both chemical and physical aspects. Indeed, acetylation lowered the grape stalks polarity, thus improving the chemical bond between PBS and GS and it also enhanced the grape stalk roughness, thus promoting physical interconnections between polymer and fillers. In addition, untreated grape stalks overall exhibited a good adhesion within PBS, though in this case, cap-shaped cavities caused by particles which had not bonded well, were also detected.

In order to quantify the adhesion, the empirical B adhesion factor was extrapolated by applying Pukanzky's equation on the experimental data. This factor increases in parallel with the increase of the particle-matrix adhesion and approaches zero for scarcely compatible particles. The untreated GS continued to show positive B values (0.99) and

512 the surface treatments enhanced the particle-matrix adhesion (Table 3). In particular,
513 PBS 10AcGS showed the highest B value (2.07), thus highlighting the efficiency of the
514 acetylation treatment.
515 PBS 10SilSituGS showed the highest tensile strength (σ_M) value among the other filled
516 composites, but, again, this result is mainly due to the lower actual content of filler
517 within the PBS matrix. Indeed, composites' tensile strength generally decreases by
518 increasing the filler loading and *vice versa* (Fu et al., 2008). Therefore, to compare the
519 adhesion effectiveness of this formulation it is useful to refer, once more, to the
520 Pukanszky's B empirical factor. In the case of PBS 10SilSituGS, the B value is 1.52
521 which is higher than PBS 10GS (0.99) but lower than PBS samples filled with treated
522 grape stalks. In other words, the grafting reaction of silane in reactive extrusion
523 improved the filler-matrix adhesion but did not do so as effectively as the direct
524 functionalization of the grape stalks.
525
526 ***3.4. Dynamic mechanical analysis***
527 In order to thoroughly evaluate the reinforcement effect of GS, dynamic mechanical
528 analysis (DMA) was also performed. The results were consistent with the tensile
529 properties. In Fig. 4a the storage modulus (E') of each PBS-based sample is reported as
530 a function of the temperature ranging from 0 °C to 100 °C. Filled samples showed
531 enhanced E' values, especially in the range 0-50 °C, while in the range 50-100 °C the
532 gap seemed to decrease, especially when comparing PBS 10GS and PBS proc.
533 Nevertheless, it is noteworthy to underline that PBS 10AcGS and silylated stalks
534 guarantee E' increments of nearly 15% even at temperatures ranging from 80 to as high
535 as 100 °C.

Fig. 4b shows the diagram of the relationship between tan δ and temperature in a range of -40 to 0 °C. The glass transition temperature (T_g), defined as the temperature at which the maximum tan δ value is observed, was only slightly enhanced by the GS fillers, shifting approximately from -20 to -19 °C. This information, combined with the fact that also the highest tan δ value showed only a moderate increase proves an effective interfacial adhesion that reduced the PBS chain mobility (Leszczyńska et a., 2018).

Nevertheless, it could be suggested that the volume of the constrained chains was not too significant. This hypothesis is indeed supported by the thermal properties, reported in Table 1, where no significant variations in the melting temperature (T_m) and in the crystallinity percentage (χ) were observed. In fact, in the case of important flexibility reductions, T_m of filled samples would have been higher than the one observed in pure PBS and c would have been lower (Giubilini et al., 2020).

3.5. Color Measurements

The visual analysis of the specimens highlighted a clear chromatic difference with the naked eye (Fig. 5a). The results of the colorimetric evaluation using the CIELab (L*, a*, b*) color space are shown in Table S3. The most interesting results were the remarkably lower ($p \leq 0.001$) L*, a*, and b* values shown by the acetylated samples (powder and specimens) in comparison with the ones related to the controls and silylated samples. This further confirms the strong alteration that occurred during the acetylation reaction in comparison with the silylated one. In the CIELab color space, L* is used to indicate the brightness, while the positive-negative a* is the redness-greenness index and the positive-negative b* the yellowness-blueness one.

560 The colorimetric evaluation was also carried out considering the determination of the
561 color indices chroma and hue (Table S3). The chroma corresponds to the colorfulness of
562 an area judged in proportion to the brightness and this color index was higher for the
563 powder as it is and for the silylated sample as compared to the acetylated sample.
564 Similarly, the bio-composites obtained from the powders as they are and from the
565 silylated ones had higher chroma values than those deriving from acetylated samples.
566 The hue is the attribute of a visual perception according to which an area appears to be
567 similar to one, or to proportions of two, of the perceived colors, red, yellow, green, and
568 blue. In the powders and in the biocomposite specimens this index was lower for
569 acetylated samples than for the control and the silylated ones. For this reason, the color
570 distances showed higher values when comparing the acetylated powders and specimens
571 with the corresponding remainder (Fig. 5b and 5c). When the color distance exceeds the
572 threshold value of 5, the human eye is capable of perceiving a color difference between
573 two objects (Musetti et al., 2015).
574 The differences in the values of chroma and hue were due to the fact that in the
575 acetylation reaction there was an increase in the carbon content, which caused a
576 decrease in brightness and hue (Cai et al., 2019). In fact, carbon was also added with
577 silanization and the reduced color distance when compared to the controls could be
578 further confirmation of the partial functionalization.
579

580 **4. Conclusions**

581 In this work, the possible valorization of grape stalks' by-products as newly-evaluated,
582 cost-advantageous and natural reinforcing fillers within poly(butylene succinate) (PBS)
583 was ascertained. Among all tested grape stalks-derived fillers, acetylated grape stalks

584 (AcGS) showed the best mechanical performance. Indeed, as confirmed by FT-IR and
585 SEM-FEG analyses, the acetylation reaction rendered the surface of grape stalks more
586 hydrophobic, as well as rougher and spongier. The combination of these chemical and
587 physical modifications resulted in a good particle-polymer matrix adhesion which led to
588 satisfactory mechanical properties.
589 Aside from the improved mechanical properties, the incorporation of 10-phr grape stalk
590 powder into a biodegradable polymer as polybutylene succinate leads to reduced use of
591 the polymer and thus lowers the cost of the finished material besides providing several
592 different woody hues. It also permits the valorization of by-products derived from the
593 wine industry such as grape stalks which are usually accumulated in huge quantities and
594 also represent a high cost in terms of disposal. This project could, therefore, have a
595 strong impact on the circular economy in pushing it to study and make use of
596 biomaterials derived from food waste.
597

598 **Acknowledgments**

599 This work was supported by the Emilia-Romagna Region, Italy, [grant number CUP
600 E81I18003220009 *Bando Alte Competenze*, "Recovery of useful molecules from low-
601 value waste of the wine industry" (Ref. PA: 2016-8349/RER), PO FSE 2014-2020
602 "Safety, Quality and Integration of regional agri-food chains to increase their
603 competitiveness"].
604 The authors wish to thank Dr. Sara Ronconi (English-language reviewer) for her
605 valuable contribution to the drafting of the present article. Moreover, we thank the Bank
606 Foundation "Cassa di Risparmio di Modena" for the FT−IR and SEM-FEG instruments
607 used in the CIGS Interdepartmental Centre of the University of Modena and Reggio

608 Emilia, as well as Dr Fabio Bergamini and Dr Massimo Tonelli for their advice and
609 valuable support. We thank the C.R.P.A. lab (Technopole of Reggio Emilia) for the use
610 of the Pulverisette 19 mill.
611

612 **Conflict of Interest Statement**

613 The authors declare that there is no conflict of interest regarding the publication of this
614 article.
615

616 **Data Availability statement**

617 The raw/processed data required to reproduce these findings cannot be shared at this
618 time as the data is also part of an ongoing study.
619

References

Abdellaoui, H., Bouhfid, R., Qaiss, A.E.K., 2018. Lignocellulosic fibres reinforced thermoset composites: preparation, characterization, mechanical and rheological properties, in: S. Kalia (Ed.), Lignocellulosic Composite Materials, Springer, Cham, Switzerland, pp. 215–270. https://doi.org/10.1007/978-3-319-68696-7_5

Ahankari, S.S., Mohanty, A.K., Misra, M., 2011. Mechanical behaviour of agro-residue reinforced poly (3-hydroxybutyrate-co-3-hydroxyvalerate),(PHBV) green composites: A comparison with traditional polypropylene composites. Compos. Sci. Technol. 71(5) 653–657. https://doi.org/10.1016/j.compscitech.2011.01.007

Barba, F.J., Zhu, Z., Koubaa, M., Sant'Ana, A.S., Orlien, V., 2016. Green alternative methods for the extraction of antioxidant bioactive compounds from winery wastes and by-products: A review. Trends Food Sci. Technol. 49, 96–109. https://doi.org/10.1016/j.tifs.2016.01.006

Battegazzore, D., Noori, A, Frache, A., 2019. Natural wastes as particle filler for poly (lactic acid)-based composites. J. Compos. Mater. 53(6) 783–797. https://doi.org/10.1177%2F0021998318791316

Bevilacqua, N., Morassut, M., Serra, M.C., Cecchini, F., 2017. Determinazione dell'impronta carbonica dei sottoprodotti della vinificazione e loro valenza biologica. Ingegneria dell'Ambiente 4(3), 277–285. http://dx.doi.org/10.14672/ida.v4i3.1142

Bharath, K.N., Basavarajappa, S., 2016. Applications of biocomposite materials based on natural fibers from renewable resources: a review. Sci. Eng. Compos. Mater. 23(2), 123–133. https://doi.org/10.1515/secm-2014-0088

Borsoi, C. Menin, C., Lavoratti, A., Zattera, A.J., 2019. Grape stalk fibers as reinforcing filler for polymer composites with a polystyrene matrix. J. Appl. Polym. Sci. 136(18), 47427. https://doi.org/10.1002/app.47427

Brandt, A., Gräsvik, J., Hallett, J.P. Welton, T., 2013. Deconstruction of lignocellulosic biomass with ionic liquids. Green Chem. 15(3), 550–583. https://doi.org/10.1039/C2GC36364J

Brostow, W., Datashvili, T., Jiang, P., Miller, H., 2016. Recycled HDPE reinforced with sol–gel silica modified wood sawdust. Eur. Polym. J. 76, 28–39. https://doi.org/10.1016/j.eurpolymj.2016.01.015

Cai, S., Zhang, N., Li, K., Li, Y., Wang, X., Nantong, P.R., 2019. Effect of pressurized hot water treatment on the mechanical properties, surface color, chemical composition and crystallinity of pine wood. Wood Research 64(3), 389–400. http://www.woodresearch.sk/wr/201903/02.pdf (accessed 19 January 2021).

Cancelli, U., Montevecchi, G., Masino, F., Mayer-Laigle, C., Rouau, X., Antonelli, A., 2020. Grape stalk: a first attempt to disentangle its fibres via electrostatic separation. Food Bioprod. Process. 124, 455–468. https://doi.org/10.1016/j.fbp.2020.10.006

Chrissafis, K., Paraskevopoulos, K., Bikiaris, D., 2005. Thermal degradation mechanism of poly (ethylene succinate) and poly (butylene succinate): comparative study. Thermochim. Acta 435(2), 142–150. https://doi.org/10.1016/j.tca.2005.05.011

Cousins, W., 1978. Young's modulus of hemicellulose as related to moisture content. Wood Sci. Technol. 12(3), 161–167. https://doi.org/10.1007/BF00372862

Espert, A., Camacho, W., Karlson, S., 2003. Thermal and thermomechanical properties of biocomposites made from modified recycled cellulose and recycled polypropylene. J. Appl. Polym. Sci. 89(9), 2353–2360. https://doi.org/10.1002/app.12091

662 Fortea-Verdejo, M., Bumbaris, E., Burgstaller, C., Bismarck, A., Lee, K.Y., 2017. Plant fibre-reinforced
663 polymers: where do we stand in terms of tensile properties? Int. Mater. Rev. 62(8), 441–464.
664 https://doi.org/10.1080/09506608.2016.1271089

665 Fu, S.Y., Feng, X.Q., Lauke, B., Mai, Y.W., 2008. Effects of particle size, particle/matrix interface
666 adhesion and particle loading on mechanical properties of particulate–polymer composites. Composites
667 Part B 39(6), 933–961. https://doi.org/10.1016/j.compositesb.2008.01.002

668 Ghaffar, S.H., Fan, M., McVicar, B., 2015. Bioengineering for utilisation and bioconversion of straw
669 biomass into bio-products. Ind. Crops Prod. 77, 262–274. https://doi.org/10.1016/j.indcrop.2015.08.060

670 Giubilini, A., Sciancalepore, C., Messori, M., Bondioli, F., 2020. New biocomposite obtained using
671 poly(3-hydroxybutyrate-co-3-hydroxyhexanoate) (PHBH) and microfibrillated cellulose. J. Appl. Polym.
672 Sci. 137(32), 48953. https://doi.org/10.1002/app.48953.

673 Gurunathan, T., Mohanty, S., Nayak, S.K., 2015. A review of the recent developments in biocomposites
674 based on natural fibres and their application perspectives. Compos. Part A Appl. Sci. Manuf. 77, 1–25.
675 https://doi.org/10.1016/j.compositesa.2015.06.007

676 Gustavsson, J., Cederberg, C., Sonesson, U., Van Otterdijk, R., Meybeck, A., 2011. Global Food Losses
677 and Food Waste. FAO, Rome, pp. 1–38.

678 Gwon, J.G., Lee, S.Y., Doh, G.H., Kim, J.H., 2010a. Characterization of chemically modified wood fibers
679 using FTIR spectroscopy for biocomposites. J. Appl. Polym. Sci. 116(6), 3212–3219.
680 https://doi.org/10.1002/app.31746

681 Gwon, J.G., Lee, S.Y., Chun, S.J., Doh, G.H., Kim, J.H., 2010b. Effects of chemical treatments of hybrid
682 fillers on the physical and thermal properties of wood plastic composites. Composites Part A 41(10),
683 1491–1497. https://doi.org/10.1016/j.compositesa.2010.06.011

684 Hajiha, H., Sain, M., Mei, L.H., 2014. Modification and characterization of hemp and sisal fibers. J. Nat.
685 Fibers 11(2), 144–168. https://doi.org/10.1080/15440478.2013.861779

686 Halpin, J.C., 1969. Stiffness and expansion estimates for oriented short fiber composites. J. Composite
687 Materials 3(4), 732–734. https://doi.org/10.1177%2F002199836900300419

688 Hernandez Michelena, A., 2019. Natural fibre reinforced composite materials, PhD Thesis (University of
689 Plymouth).

690 Hunt, R.W.G., Pointer, M.R., 2011. Measuring Colour, fourth ed. Wiley & Sons, New York (USA).

691 Hussain, M.A., 2004. Alternative routes of polysaccharide acylation: synthesis, structural analysis,
692 properties, PhD Thesis (Friedrich-Schiller-Universität Jena).

693 Jarvis, M.C., 2018. Structure of native cellulose microfibrils, the starting point for nanocellulose
694 manufacture. Philos. Trans. R. Soc. London, Ser. A. 376, 20170045.
695 https://doi.org/10.1098/rsta.2017.0045

696 Kai, W., He, Y., Inoue, Y., 2005. Fast crystallization of poly(3-hydroxybutyrate) and poly(3-
697 hydroxybutyrate-co-3-hydroxyvalerate) with talc and boron nitride as nucleating agents. Polym. Int.
698 54(5), 780–789. https://doi.org/10.1002/pi.1758

699 Kalia, S., Thakur, K., Celli, A., Kiechel, M.A., Schauer, C.L., 2013. Surface modification of plant fibers
700 using environment friendly methods for their application in polymer composites, textile industry and
701 antimicrobial activities: A review. J. Environ. Chem. Eng. 1(3), 97–112.
702 https://doi.org/10.1016/j.jece.2013.10.011

703 Leszczyńska, A., Stafin, K., Pagacz, J., Mičušík, M., Omastova, M., Hebda, E., Pielichowski, J.,
704 Borschneck, D., Rose, J., Pielichowski, K., 2018. The effect of surface modification of microfibrillated

cellulose (MFC) by acid chlorides on the structural and thermomechanical properties of biopolyamide 4.10 nanocomposites. Ind. Crops Prod. 116, 97–108. https://doi.org/10.1016/j.indcrop.2018.02.022

Le Troedec, M., Sedan, D., Peyratout, C., Bonnet, J.P., Smith, A., Guinebretiere, R., Gloaguenc, V., Krausz, P., 2008. Influence of various chemical treatments on the composition and structure of hemp fibres. Compos. Part A Appl. Sci. Manuf. 39(3), 514–522. https://doi.org/10.1016/j.compositesa.2007.12.001

Li, X., Tabil, L.G., Panigrahi, S., 2007. Chemical treatments of natural fiber for use in natural fiber-reinforced composites: a review. J. Polym. Environ 15(1), 25–33. 10.1007/s10924-006-0042-3

Lieder, M., Rashid, A., 2016. Towards circular economy implementation: a comprehensive review in context of manufacturing industry. J. Clean. Prod., 115, 36–51. https://doi.org/10.1016/j.jclepro.2015.12.042

Lucarini, M., Durazzo, A. Romani, A., Campo, M., Lombardi-Boccia, G., Cecchini, F., 2018. Bio-based compounds from grape seeds: A biorefinery approach. Molecules. 23(8), 1888. doi:10.3390/molecules23081888

Luzi, F., Torre, L., Kenny, J.M., Puglia, D., 2019. Bio-and fossil-based polymeric blends and nanocomposites for packaging: Structure–property relationship. Materials. 12(3), 471. https://doi.org/10.3390/ma12030471

MacArthur, E., 2013. Towards the Circular Economy: Opportunities for the Consumer Goods Sector, Ellen MacArthur Foundation, Cowes, UK.

Maicas, S., Mateo, J.J., 2020. Sustainability of Wine Production. Sustainability. 12(2), 559. https://doi.org/10.3390/su12020559

Maina, S., Kachrimanidou, V., Koutinas, A., 2017. A roadmap towards a circular and sustainable bioeconomy through waste valorization. Curr. Opin. Green Sustainable Chem. 8, 18–23. https://doi.org/10.1016/j.cogsc.2017.07.007

Masino, F. Chinnici, F., Bendini, A., Montevecchi, G., Antonelli, A., 2008. A study on relationships among chemical, physical, and qualitative assessment in traditional balsamic vinegar. Food Chem. 106(1), 90–95. https://doi.org/10.1016/j.foodchem.2007.05.069

McLaren, K., 1976. XIII—The development of the CIE 1976 (L* a* b*) uniform colour space and colour-difference formula. J. Soc. Dyers Colourists 92(9), 338–341. https://doi.org/10.1111/j.1478-4408.1976.tb03301.x

Mohammed-Ziegler, I. Tánczos, I., Hórvölgyi, Z., Agoston, B., 2008. Water-repellent acylated and silylated wood samples and their surface analytical characterization. Colloids Surf. A Physicochem. Eng. Asp. 319(1-3), 204–212. https://doi.org/10.1016/j.colsurfa.2007.06.063

Montevecchi, G., Masino, F., Antonelli, A., 2011. Pyroglutamic acid development during grape must cooking. Eur. Food Res. Technol. 232(2), 375–379. https://doi.org/10.1007/s00217-010-1383-7

Montevecchi, G., Simone Vasile, G., Matrella, V., Masino, F., Imazio, S. A., Antonelli, A., Bignami, C., 2014. Study of anthocyanin profile for valorization of autochthonous grapevine (Vitis vinifera L.) cultivars of the Emilia Romagna region, in: Warner, L.M. (Ed.), Handbook of Anthocyanins: Food Sources, Chemical Applications and Health Benefits. Nova Science Publishers Inc., Hauppauge, USA, pp. 197–216.

Mu, B., Wang, H., Hao, X., Wang. Q., 2018. Morphology, mechanical properties and dimensional stability of biomass particles/high density polyethylene composites: Effect of species and composition. Polymers. 10(3), 308. https://doi:10.3390/polym10030308

748 Musetti, A., Tagliazucchi, D., Montevecchi, G., Verzelloni, E., Antonelli, A., Fava, P., 2015.
749 Characterization of a combined treatment with alpha-lipoic acid for the control of enzymatic browning in
750 fresh-cut golden Delicious apples. J. Food Process. Preserv. 39(6), 681–687.
751 https://doi.org/10.1111/jfpp.12276

752 Nabinejad, O., Sujan, D., Rahman, M.E., Davies, I.J., 2015. Determination of filler content for natural
753 filler polymer composite by thermogravimetric analysis. J. Therm. Anal. Calorim. 122(1), 227–233.
754 https://doi.org/10.1007/s10973-015-4681-2

755 Nanni, A., Messori, M., 2020a. Effect of the wine lees wastes as cost-advantage and natural fillers on the
756 thermal and mechanical properties of poly (3-hydroxybutyrate-co-hydroxyhexanoate)(PHBH) and poly
757 (3-hydroxybutyrate-co-hydroxyvalerate)(PHBV). J. Appl. Polym. Sci. 137(28), 48869.
758 https://doi.org/10.1002/APP.48869

759 Nanni, A., Messori, M., 2020b. Thermo-mechanical properties and creep modelling of wine lees filled
760 Polyamide 11 (PA11) and Polybutylene succinate (PBS) bio-composites. Compos. Sci. Technol. 188,
761 107974. https://doi.org/10.1016/j.compscitech.2019.107974

762 Nanni, A., Ricci, A., Versari, A., Messori, M., 2020. Wine derived additives as poly (butylene
763 succinate)(PBS) natural stabilizers for different degradative environments. Polym. Degrad. Stabil. 182,
764 109381. https://doi.org/10.1016/j.polymdegradstab.2020.109381

765 Nanni, A., Parisi, M., Colonna, M., 2021. Wine by-products as raw materials for the production of
766 biopolymers and of natural reinforcing fillers: a critical review. Polymers 13(3) 381.
767 https://doi.org/10.3390/polym13030381

768 Parisi, M., Nanni, A., Colonna, M., 2021. Recycling of chrome-tanned leather and its utilization as
769 polymeric materials and in polymer-based composites: a review. Polymers 13(3), 429.
770 https://doi.org/10.3390/polym13030429

771 Pickering, K.L., Beckermann, G.W., Alam, S.N., Foreman, N.J., 2007. Optimising industrial hemp fibre
772 for composites. Compos Part A Appl Sci Manuf. 38(2), 461–468.
773 https://doi.org/10.1016/j.compositesa.2006.02.020

774 Prozil, S.O., Evtuguin, D.V., Lopes, L.P.C., 2012. Chemical composition of grape stalks of Vitis vinifera
775 L. from red grape pomaces. Ind. Crops Prod. 35(1), 178–184.
776 https://doi.org/10.1016/j.indcrop.2011.06.035

777 Prozil, S.O., Evtuguin, D.V., Silva, A.M.S., Lopes, L.P.C., 2014. Structural characterization of lignin
778 from grape stalks (Vitis vinifera L.). J Agric. Food Chem. 62(24), 5420–5428.
779 https://doi.org/10.1021/jf502267s

780 Pukanszky, B., 1990. Influence of interface interaction on the ultimate tensile properties of polymer
781 composites. Composites 21(3), 255–262. https://doi.org/10.1016/0010-4361(90)90240-W

782 Ramiah, M., 1970. Thermogravimetric and differential thermal analysis of cellulose, hemicellulose, and
783 lignin. J. Appl. Polym. Sci 14(5), 1323–1337. https://doi.org/10.1002/app.1970.070140518

784 Ravindran, R., Jaiswal, A.K., 2016. Exploitation of food industry waste for high value products. Trends
785 Biotechnol. 34(1), 58–69. https://doi.org/10.1016/j.tibtech.2015.10.008

786 Ronga, D., Francia, E., Allesina, G., Pedrazzi, S., Zaccardelli, M., Pane, C., Tava, A., Bignami, C., 2019.
787 Valorization of vineyard by-products to obtain composted digestate and biochar suitable for nursery
788 grapevine (Vitis vinifera L.) production. Agronomy (Basel). 9(8), 420.
789 https://doi.org/10.3390/agronomy9080420

Saba, N., Jawaid, M., Alothman, O.Y., Paridah, M.T., 2016. A review on dynamic mechanical properties of natural fibre reinforced polymer composites. Constr. Build. Mater. 106, 149–159. https://doi.org/10.1016/j.conbuildmat.2015.12.075

Sahoo, S., Misra, M., Mohanty, A.K., 2011. Enhanced properties of lignin-based biodegradable polymer composites using injection moulding process. Composites Part A 42(11), 1710–1718. https://doi.org/10.1016/j.compositesa.2011.07.025

Sawpan, M.A., Pickering, K.L., Fernyhough, A., 2011. Effect of various chemical treatments on the fibre structure and tensile properties of industrial hemp fibres. Compos. Part A Appl. Sci. Manuf. 42(8), 888–895. https://doi.org/10.1016/j.compositesa.2011.03.008

Seggiani, M., Cinelli, P., Verstichel, S., Puccini, M., Vitolo, S., Anguillesi, I., Lazzeri, A., 2015. Development of fibres-reinforced biodegradable composites. Chem. Eng. Trans. 43, 1813–1818. https://doi.org/10.3303/cet1543303

Seggiani, M., Cinelli, P., Geicu, M., Popa, M.E., Puccini, M., Lazzeri, A., 2016. Microbiological valorisation of bio-composites based on polylactic acid and wood fibres. Chem. Eng. Trans. 49, 127–132. https://doi.org/10.3303/cet1649022

Seggiani, M., Cinelli, P., Mallegni, N., Balestri, E., Puccini, M., Vitolo, S., Lardicci, C., Lazzeri, A., 2017. New bio-composites based on polyhydroxyalkanoates and Posidonia oceanica fibres for applications in a marine environment. Materials (Basel). 10(4), 326. https://doi.org/10.3390/ma10040326

Spigno, G., Maggi, L., Amendola, D., Dragoni, M., De Faveri, D.M., 2013. Influence of cultivar on the lignocellulosic fractionation of grape stalks. Ind. Crops Prod. 46, 283–289. https://doi.org/10.1016/j.indcrop.2013.01.034

Stegmann, P., Londo, M. Junginger, M., 2020. The circular bioeconomy: its elements and role in European bioeconomy clusters. Resour. Conserv. Recycl. X. 6, 100029. https://doi.org/10.1016/j.rcrx.2019.100029

Suardana, N., Piao, Y., Lim, J.K., 2011. Mechanical properties of hemp fibers and hemp/pp composites: effects of chemical surface treatment. Materials Physics and Mechanics 11(1), 1–8.

Then, Y.Y., Ibrahim, N.A., Zainuddin, N., Ariffin, H., Yunus, W., Zin, W.M., 2013. Oil palm mesocarp fiber as new lignocellulosic material for fabrication of polymer/fiber biocomposites. Int. J. Polym. Sci. 2013, 797452. https://doi.org/10.1155/2013/797452

Troncozo, M.I., Lješević, M., Beškoski, V.P., Anđelković, B., Balatti, P.A., Saparrat, M.C., 2019. Fungal transformation and reduction of phytotoxicity of grape pomace waste. Chemosphere. 237, 124458. https://doi.org/10.1016/j.chemosphere.2019.124458

Tserki, V., Zafeiropoulos, N.E., Simon, F., Panayiotou, C., 2005. A study of the effect of acetylation and propionylation surface treatments on natural fibres. Compos. Part Aappl. Sci. Manuf. 36(8), 1110–1118. https://doi.org/10.1016/j.compositesa.2005.01.004

Väisänen, T., Das, O., Tomppo, L., 2017. A review on new bio-based constituents for natural fiber-polymer composites. J. Clean. Prod. 149, 582–596. https://doi.org/10.1016/j.jclepro.2017.02.132

Vasile Simone, G. Montevecchi, G., Masino, F., Matrella, V., Imazio, S.A., Antonelli, A. Bignami, C., 2013. Ampelographic and chemical characterization of Reggio Emilia and Modena (northern Italy) grapes for two traditional seasonings: ‘saba’ and ‘agresto’. J. Sci. Food Agric. 93(14), 3502–3511. https://doi.org/10.1002/jsfa.6296

Voigt, W., 1889. Ueber die Beziehung zwischen den beiden Elasticitätsconstanten isotroper Körper. Ann. Phys. 274(12), 573–587. https://doi.org/10.1002/andp.18892741206

WHO, 2012. S.3.6. Bulk density and tapped density of powders, Document QAS/11.450 Final, March 2012.

Xu, J., Guo, B.H., 2010. Poly (butylene succinate) and its copolymers: research, development and industrialization. Biotechnol. J. 5(11), 1149–1163. https://doi.org/10.1002/biot.201000136

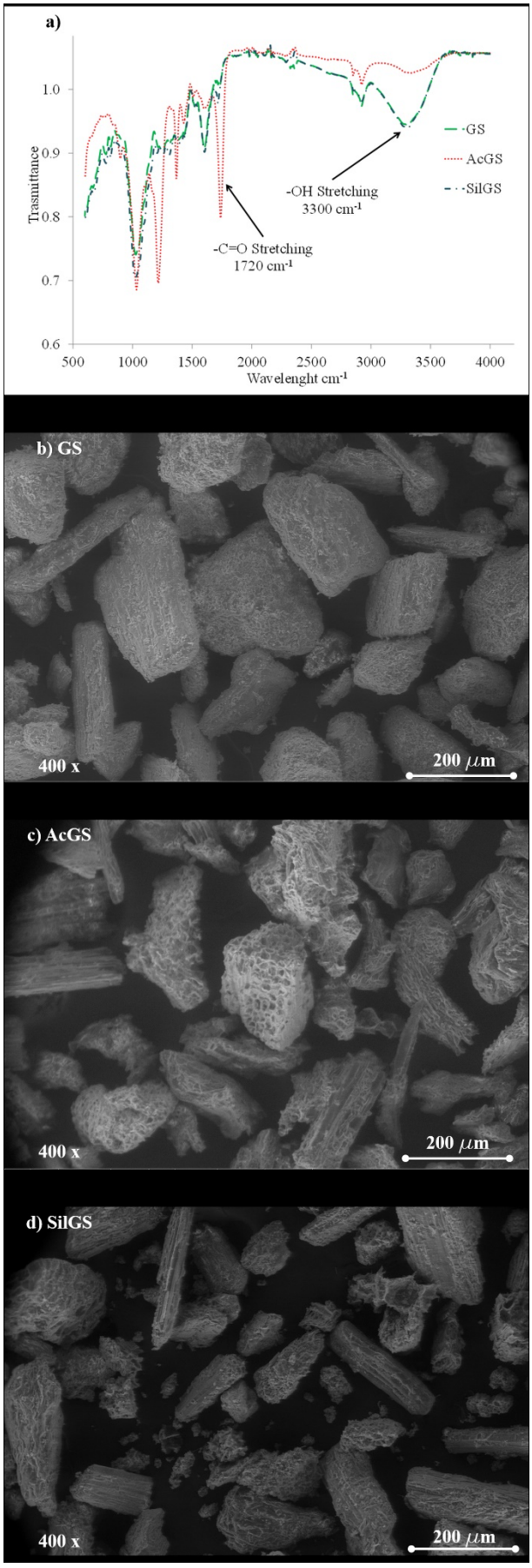
Yeh, A.I., Huang Y.C., Chen, S.H., 2010. Effect of particle size on the rate of enzymatic hydrolysis of cellulose. Carbohyd. Polym. 79(1), 192–199. https://doi.org/10.1016/j.carbpol.2009.07.049

Yim, H., Haselbeck, R., Niu, W., Pujol-Baxley, C., Burgard, A., Boldt, J., Khandurina, J., Trawick, J.D., Osterhout, R.E., Stephen, R., Estadilla, J., Teisan, S., Schreyer, H.B., Andrae, S., Yang, T.H., Lee, S.Y., Burk, M.J., Van Dien, S., 2011. Metabolic engineering of Escherichia coli for direct production of 1,4-butanediol. Nat. Chem. Biol. 7(7), 445–452. https://doi.org/10.1038/nchembio.580

Zeikus, J.G., Jain, M.K., Elankovan, P., 1999. Biotechnology of succinic acid production and markets for derived industrial products. Appl. Microbiol. Biotechnol. 51(5), 545–552. https://doi.org/10.1007/s002530051431

Zhang, Q., Shi, L., Nie, J., Wang, H., Yang, D., 2012. Study on poly (lactic acid)/natural fibers composites. J. Appl. Polym. Sci. 125(S2), E526–E533. https://doi.org/10.1002/app.36852

Zhao, Y., Sun, H., Yang, B., Weng, Y., 2020. Hemicellulose-Based Film: Potential Green Films for Food Packaging. Polymers, 12(8), 1775. https://doi.org/10.3390/polym12081775

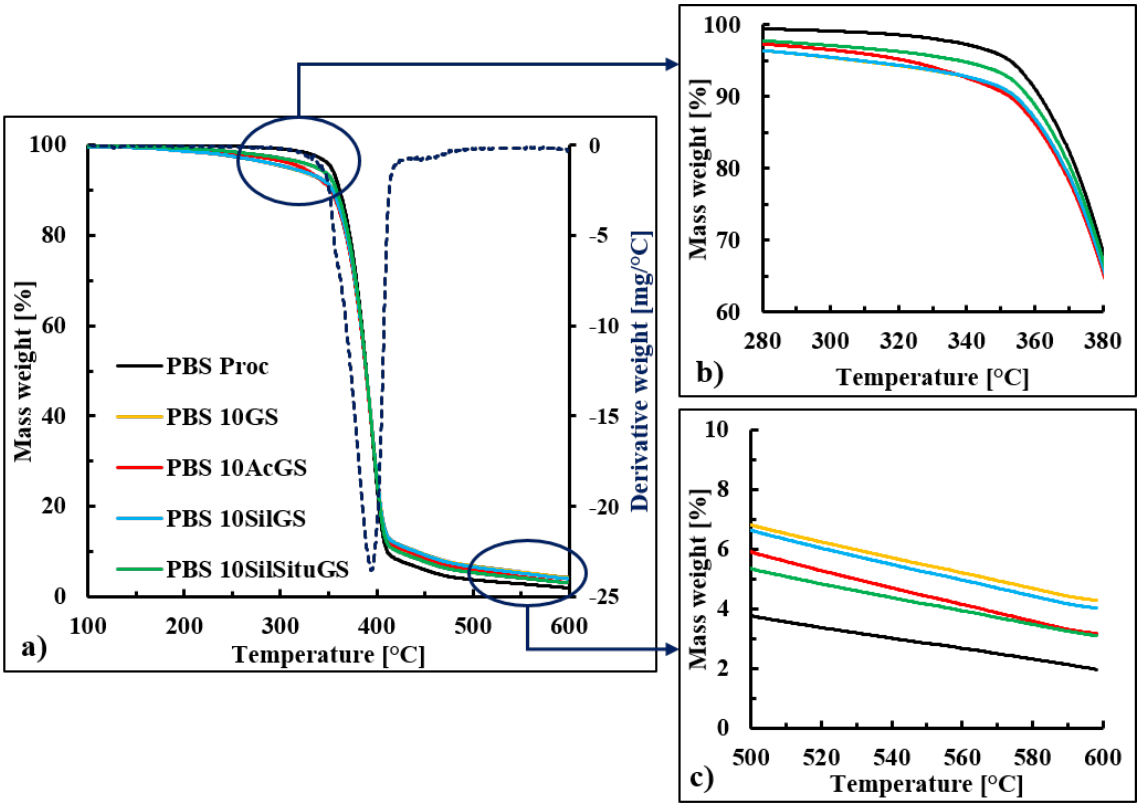

a)
Trasmittance
1.0
0.9
0.8
0.7
0.6
500
1000
1500
2000
2500
3000
3500
4000
Wavelenght cm-1
GS
AcGS
SilGS
-OH Stretching
3300 cm-1
-C=O Stretching
1720 cm-1
b) GS
400 x
200 μm
c) AcGS
400 x
200 μm
d) SilGS
400 x
200 μm

850

851 **Fig. 1**. a) FT-IR spectrum of the grape stalk powders. GS, grape stalk powder as it is; AcGS: acetylated
852 grape stalk powder; SilGS: silylated grape stalk powder. SEM-FEG images of b) untreated grape stalks
853 (GS), c) acetylated grape stalks (AcGS) and d) silylated grape stalks (SilGS).

854

855



856

857 **Fig. 2**. a) TG curves of the PBS-based composites and magnifications of 280-380 °C b) and 500-600 °C
858 c) ranges.

859

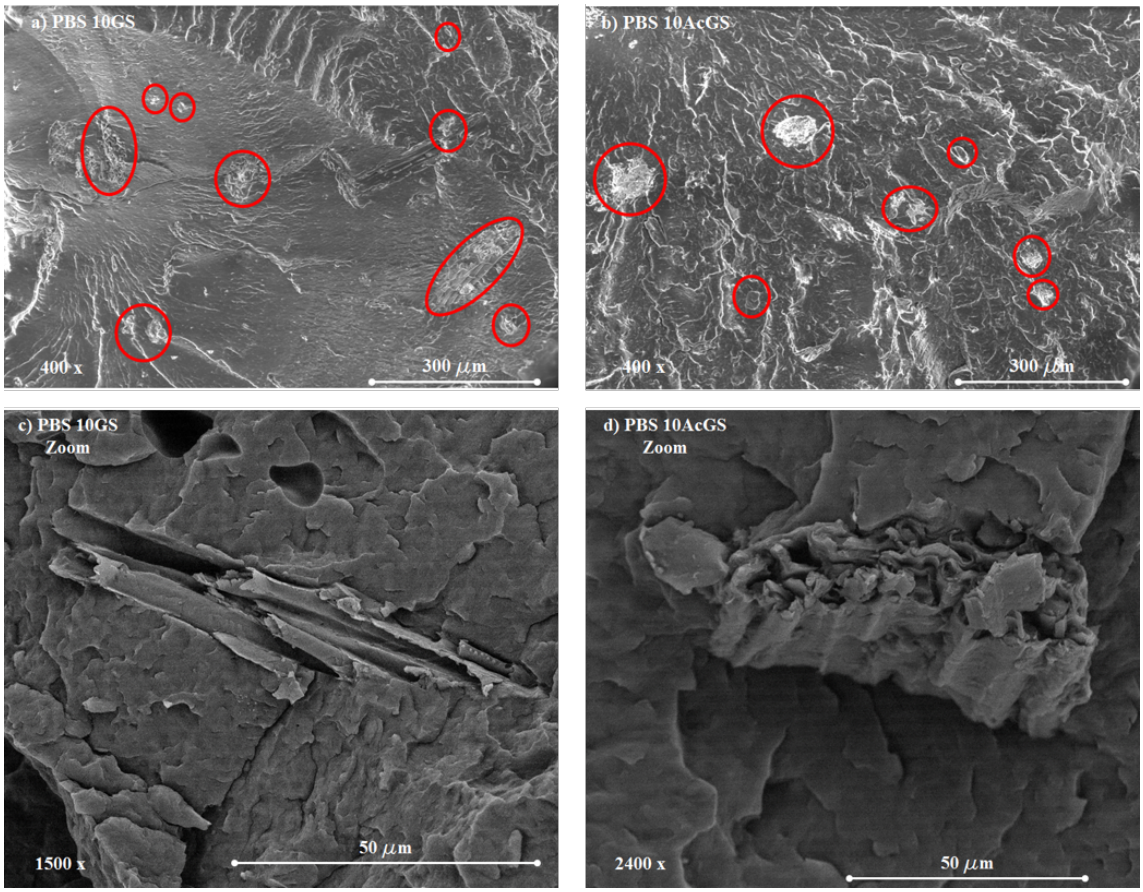
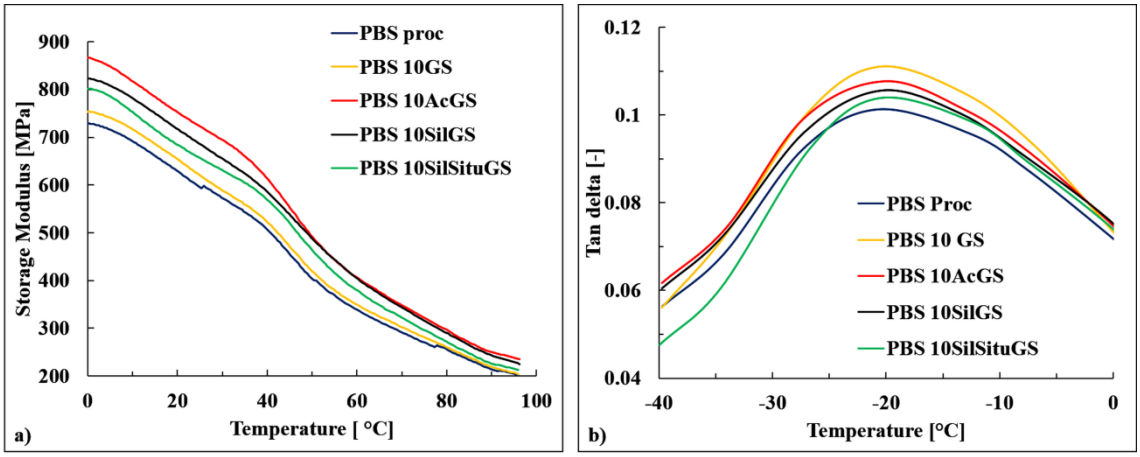


Fig. 3. SEM-FEG images of a) PBS10 GS at 400× magnification, b) PBS 10AcGS at 400× magnification, c) PBS10 GS at 1500× magnification and d) PBS 10AcGS at 2400× magnification. The red circles indicate fragments of grape stalks and give an idea of the distribution and dispersion of the filler within the polymer matrix.

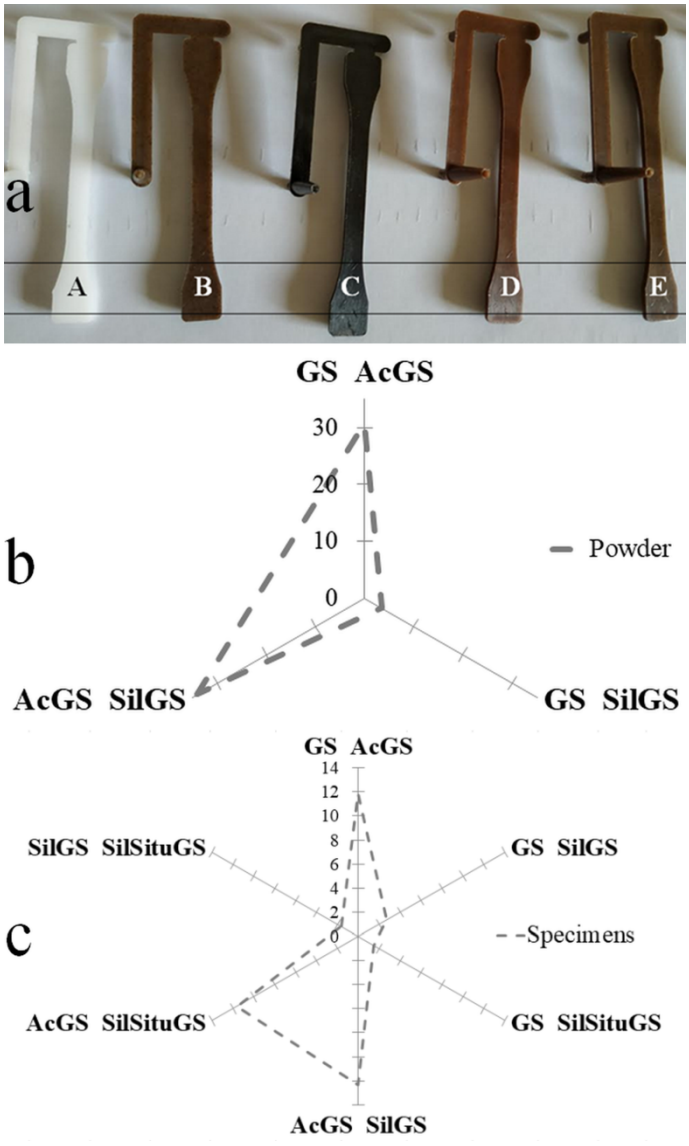
867



868

869 **Fig. 4**. Dynamic-mechanical analysis (DMA): a) storage modulus (E') and b) tan δ of the PBS based
870 samples as a function of the temperature.

871



872

873 **Fig. 5**. a) Bio-composites obtained from grape stalk powders. From left to right: (A) PBS proc specimen,
874 (B) PBS 10 phr grape stalk specimen, (C) PBS 10 phr acetylated grape stalk specimen, (D) PBS 10
875 silylated grape stalk specimen, and (E) PBS 10 silylated *in situ*. b) Color distances related to powders and
876 c) to specimens.

877 PBS, poly(butylene succinate); PBS 10GS, PBS 10 phr grape stalk specimen; PBS 10AcGS, PBS 10 phr
878 acetylated grape stalk; PBS 10SilGS, PBS 10 phr silylated grape stalk; PBS 10SilSituGS, PBS 10 phr
879 silylated *in situ* grape stalk.

880

881

Supplementary Data

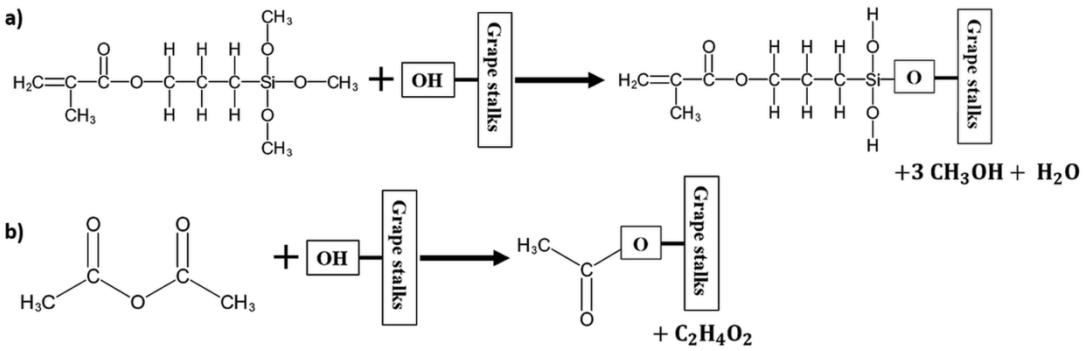


Fig. S1. Reaction scheme regarding the a) silanization and b) acetylation of the grape stalks.

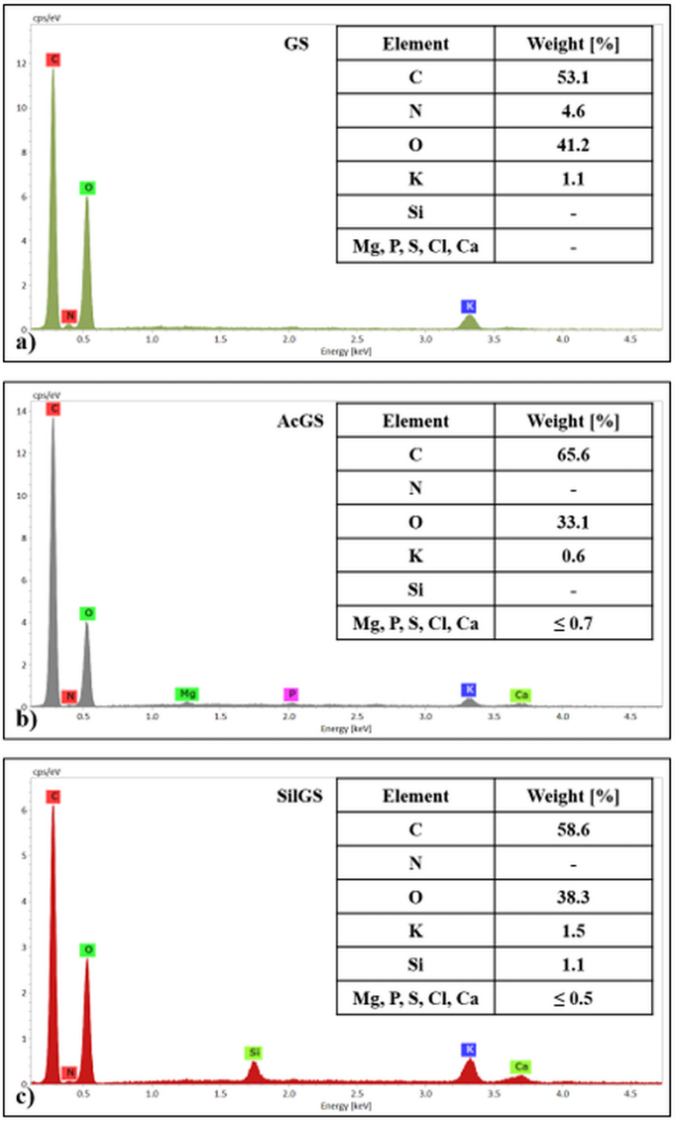


Fig. S2. X-EDS analysis of a) untreated grape stalks (GS), b) acetylated grape stalks (AcGS) and c) silylated grape stalks (SilGS).

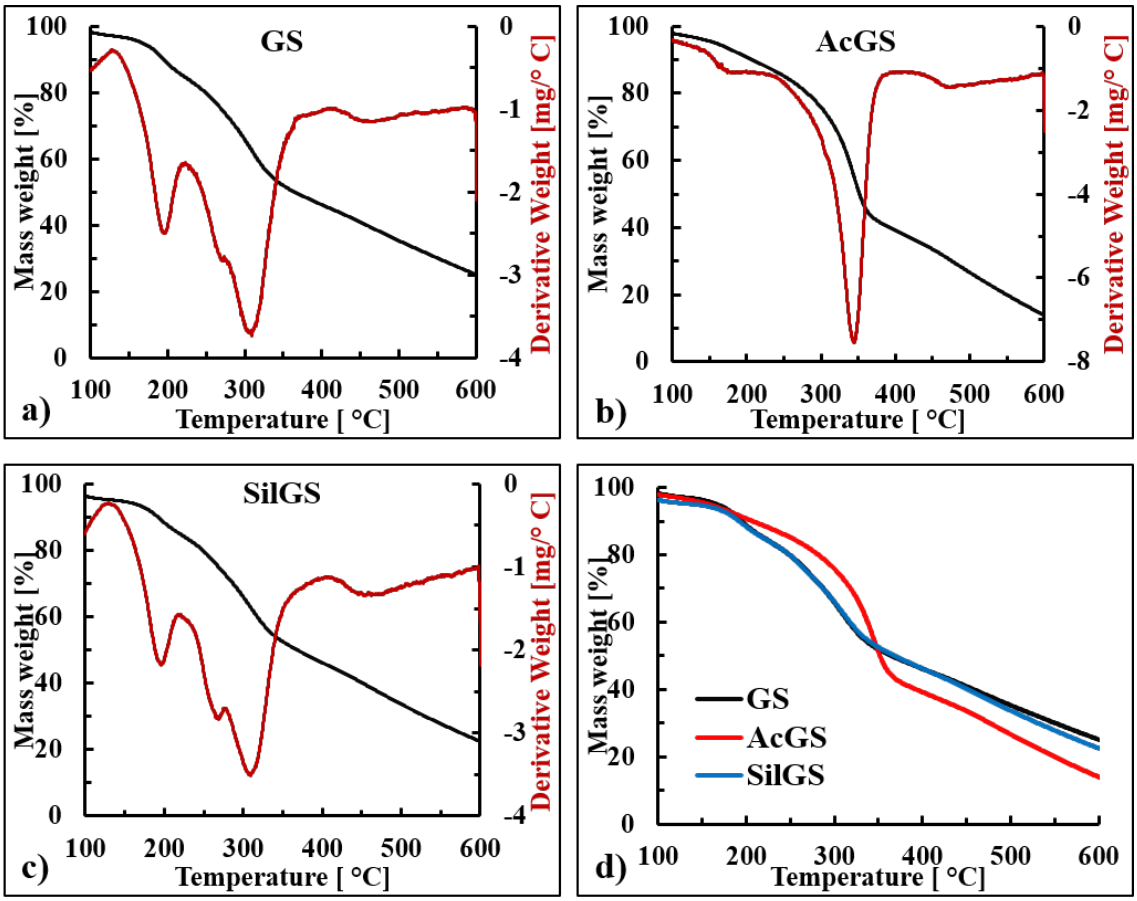


Fig. S3. TG and DT curves of a) untreated grape stalks (GS), b) acetylated grape stalks (AcGS) and c) silylated grape stalks (SilGS) and d) comparison of the TG curves of untreated and treated grape stalks.

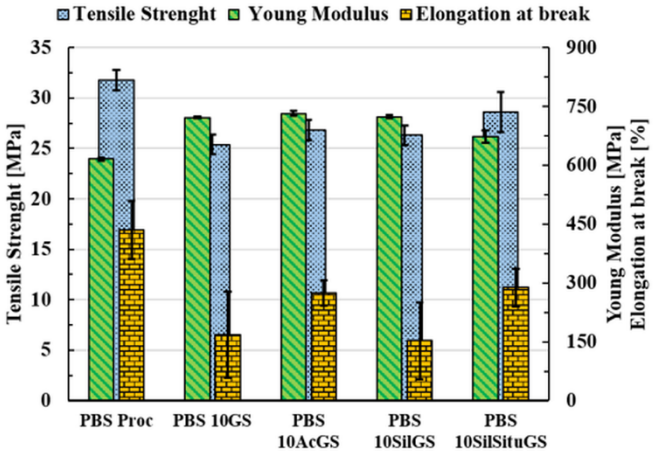


Fig. S4. Tensile properties of the PBS-based composites.

In section 2.9, a mathematical model capable to evaluating the actual filler content present within a biocomposite, exploiting TGA data of neat filler, neat polymer and resulting biocomposite was introduced. The above-mentioned model, proposed by Nabinejad *et al.*, has the following form:

$$P_f\ [\%] = \alpha * m_{dc} + \beta * R_{600,c}\ (1)$$

where P_f represents the effective mass percentage of the filler within the composite, m_{dc} is the percentage mass loss of composite evaluated at the T_{peak} of the filler, and $R_{600,c}$ is the percentage mass residue of the composite at 600 °C. The mass drop coefficient α and the mass residue coefficient β can be calculated as following:

$$\alpha\ [-] = \frac{R_{600,p}}{R_{600,p} \times M_{df} - R_{600,f} \times M_{dp}} \times 100\ (2)$$

$$\beta\ [-] = \frac{-M_{dp}}{R_{600,p} \times M_{df} - R_{600,f} \times M_{dp}} \times 100\ (3)$$

where $R_{600,f}$ and $R_{600,p}$ are the percentage mass residues evaluated at 600 °C of the neat filler and neat polymer, respectively, while M_{df} and M_{dp} are the percentage mass decreases of the neat filler and polymer evaluated at $T_{peak,f}$.

Table S1

Required TGA of the neat fillers.

	$T_{peak,f}$ [°C]	M_{df} [%]	$R_{600,f}$ [%]
GS (untreated)	308.8	37.33	23.91
Ac GS	344.0	44.48	13.91
SilGS	309.2	37.27	22.45
(SilSitu GS)	*309.0*	*37.30*	*23.18*

In the case of the formulation PBS10SilSitu GS it was not possible to determine the TGA parameters of the neat filler since the filler modification took place within the extruder (reactive extrusion). Nevertheless, it can be noticed that the TGA data (and curves) of untreated GS and SilGS are practically the same. As a consequence, the average values of GS and SilGS for $T_{peak,f}$,

M_{df} and $R_{600,f}$ were used for the composite PBS10SilSitu GS, in italics. In particular, $T_{peak,f}$ of *SilSitu GS* (309.0 °C) was used to extrapolate the m_{dc} value of the sample PBS10SilSitu GS.

In conclusion, the parameters obtained are shown in Table S2

Table S2

Values obtained by applying the model proposed by Nabinejad et al. (2015) using the TGA data of PBS composites filled with grape stalks.

	PBS 10 GS	**PBS 10AcGS**	**PBS 10SilGS**	**PBS 10SilSitu GS**
m_{dc} [%]	4.59	7.40	4.64	3.21
m_{df} [%]	37.33	44.48	37.27	37.30
m_{dp} [%]	1.05	3.22	1.07	1.06
$R_{600,c}$ [%]	4.28	3.16	4.02	3.20
$R_{600,f}$ [%]	23.91	13.91	22.45	23.18
$R_{600,p}$ [%]	1.97	1.97	1.97	1.97
α [-]	4.06	4.60	3.99	4.02
β [-]	-2.16	-7.51	-2.16	-2.16
P_f [%]	**9.41**	**10.24**	**9.80**	**6.23**

Table S3

Color analysis of the grape stalks' powders and the bio-composite specimens. Results of the one-way ANOVA and the Tukey's test applied on values are reported as Fvalues and lowercase letters, respectively. Different letters identify samples significantly different ($p \leq 0.05$).

	L*	a*	b*	C	H (°)
ANOVA (F_{values})	4952***	1654***	4984***	4698***	160***
GS powder (GS)	47.95b ± 0.60	7.95b ± 0.15	20.82b ± 0.26	22.29b ± 0.29	69.11c ± 0.16
GS acetylated powder (AcGS)	20.82a ± 0.14	3.38a ± 0.13	6.98a ± 0.25	7.75a ± 0.27	64.13a ± 0.44
GS silylated powder (SilGS)	50.34c ± 0.34	9.82c ± 0.14	22.45c ± 0.06	24.51c ± 0.01	66.38b ± 0.36
ANOVA (F_{values})	9294***	1152***	939***	1090***	37.68***
PBS proc (specimens)	76.71d ± 0.61	1.14b ± 0.12	1.20b ± 0.14	1.66b ± 0.16	46.44b ± 3.37
PBS 10GS (specimens)	34.00c ± 0.36	5.09c ± 0.24	7.69c ± 0.42	9.22c ± 0.48	56.47c ± 0.24
PBS 10AcGS (specimens)	25.79a ± 0.17	0.48a ± 0.08	0.43a ± 0.10	0.65a ± 0.12	41.47a ± 1.89
PBS 10SilGS (specimens)	32.49b ± 0.31	7.26e ± 0.12	8.31d ± 0.08	11.04e ± 0.04	48.86b ± 0.74
PBS 10SilSituGS (specimens)	32.71b ± 0.24	5.66d ± 0.14	8.18cd ± 0.20	9.95d ± 0.24	55.32c ± 0.17

GS = grape stalks; PBS = polybutylene succinate; 10GS = 10 phr of grape stalks; 10AcGS = 10 phr of acetylated grape stalks; 10SilGS = 10 phr of silylated grape stalks; 10SilSituGS = 10 phr of silylated *in situ* grape stalks. C = Chroma; H = Hue. ***$p \leq 0.001$.

Reference

Nabinejad, O., Sujan, D., Rahman, M.E., Davies, I.J., 2015. Determination of filler content for natural filler polymer composite by thermogravimetric analysis. J. Therm. Anal. Calorim. 122(1), 227–233. https://doi.org/10.1007/s10973-015-4681-2